Correlating plastic shrinkage cracking potential of fiber reinforced cement composites with its early-age constitutive response in tension

Gupta Rishi[1] and Banthia Nemkumar[2]

[1] Corresponding Author
Assistant Professor, (Civil Engineering Program),
Department of Mechanical Engineering,
University of Victoria, EOW Room # 343
Victoria B.C. (CANADA) V8W 2Y2, Tel +1 (250) 721-7033
Email: guptar@uvic.ca

[2] Professor, Distinguished University Scholar &
Canada Research Chair in Infrastructure Rehabilitation
Department of Civil Engineering, The University of British Columbia
Vancouver, B.C., CANADA

ABSTRACT

It is well understood that the early-age properties of cementitious materials influences its long-term performance. Cementitious materials experience high moisture loss at early age resulting in volumetric shrinkage. When this shrinkage is restrained, tensile stresses develop resulting in cracking of the material. This issue is more pronounced at early-age when the tensile strength of cementitious materials is not fully developed. There are many methods and models available to predict the drying shrinkage of concrete. However, the relationship between early age uniaxial tensile strength and restrained shrinkage cracking characteristics at early age is not well understood. Uniaxial tests were conducted on dog-bone specimens made using various fiber types including glass, cellulose and three types of synthetic fibers. Tensile characteristics including stress vs. strain plots for all the specimens along with stress at peak, post crack strength at 2mm deflection along with elongation at peak are calculated and presented in this paper. Plastic shrinkage cracking

results obtained using an innovative test developed by the authors were correlated to these tensile strength results. Results indicate that post crack residual tensile strength at early-age is inversely proportional to the total crack area resulting from restrained shrinkage. The effectiveness of various fiber types is also discussed in the paper.

INTRODUCTION

Early-age properties of cementitious materials play a vital role in influencing the long-term properties of the material. One important early-age property of cementitious materials is plastic shrinkage, which when restrained can lead to cracking. There are many direct methods to determine the plastic shrinkage potential of cementitious materials that are typically simple and mainly involve measurement of reduction in a certain dimension of the specimens (Kronlof et al., 1995; Kovler, 1995). These specimens are generally in the shape of a prism. Others have reported measuring shrinkage using non-contact laser (Qi et al., 2005), measuring strains using fiber bragg gratings to measure strains (Slowik et al., 2004), and relating bleeding and evaporation to plastic shrinkage cracking (Topcu & Elgun, 2004). Measurement of strain in systems that do not crack can be useful in predicting the cracking potential. As opposed to the free shrinkage tests, there are several existing techniques of studying shrinkage induced cracking in cement-based materials. These include, for example, a ring type specimen (Grzybowski & Shah, 1990), a linear specimen with anchored ends (Banthia et al., 1993), a linear specimen held between a movable and a fixed grip such that a complete restraint and one-dimensional fixity are achieved by returning the movable grip to the original position after shrinkage (Bloom & Bentur, 1995),

and a plate type specimen where the restraint is provided in two orthogonal directions (Khajuria & Balaguru, 1992).

There are many other test techniques, where a slab-type specimen is used to evaluate the plastic shrinkage cracking (Soroushian et al. (1993), Bayasi and McIntyre (2002), Naaman et al. (2005), Qi et al. (2003), Trottier et al. (2002), Lura et al. (2007), ASTM C 1579 (2006)). While effective for comparative measurements, most of the techniques described above produce stress fields in the specimen that are different from those occurring in reality, especially in the case of thin overlays. This led to the development of a test method by the authors where a layer of fresh concrete (or shotcrete) is placed directly on a fully hardened substrate. This technique is described later in this paper and was used to determine the plastic shrinkage cracking potential of a control mix and then compared to modified mixes containing fly-ash and fiber reinforcement. The restraint in this technique creates a strain differential that causes tensile stresses in the material to exceed the strength resulting in cracking. Hence, the uniaxial tensile strength of the material at the same age when plastic shrinkage cracking initiates would define the formation of cracks. When fibers are used, the post crack strength under direct tension would also be expected to have a direct influence on controlling the crack width. This effect of fibers on the uniaxial tensile characteristics in the hardened state is well documented (Meng et al. (2006), Wille et al. (2014), Körmeling and Reinhardt (1987), Akcay (2012)). However, the authors only came across one study by Aly and Sanjayan (2010) where the early-age uniaxial tension tests were conducted along with plastic shrinkage cracking measurements. However, this study only considered one type of polypropylene fiber and did not utilize a plastic shrinkage test that measures the total cracking in the specimens and rather measures the shrinkage strain

and stress only. The aim of the study described in this paper was to relate plastic shrinkage cracking potential to the early age tensile characteristics of fiber reinforced and control (unreinforced mixes).

TEST PROGRAM

Mixes

Different mixes considered in this investigation are described in Table 1. A fiber dosage (V_f) of 0.1% by volume was selected for all fiber reinforced mixes since 0.1% was the fiber dosage previously found by the authors to be the optimal (for most fibers) in controlling shrinkage cracks (Gupta, 2008). Some fiber types at 0.1% completely eliminated plastic shrinkage cracking. The detailed results of this previous study (Gupta, 2008) including average crack area, average crack width, number of cracks are reproduced in Table 2. In this table results for eight types of polypropylene fibers (designation PF), five types of cellulose fibers (designation CF) and one type of glass fiber (designation GF) is presented. These previously reported results were used for comparison to uniaxial properties in the current investigation. The properties of the various fibers used in the current investigation is presented in Table 3. The focus of this study was to evaluate the early-age tensile strength of the mixes and compare them to previously available plastic shrinkage cracking results (Table 2). Two unreinforced mixes were used as control mixes. One of the control mixes (C2) had the cement replaced by 20% fly-ash. The mixes considered in this program were mortar mixes with water-cement ratio (w/c) = 0.5, sand-cement ratio (s/c) = 0.5, and Cement = 1200kg/m^3.

Table 1- Mixes Investigated under Early-Age Uniaxial Tension

Fiber type	Mix Designation	Admixtures	V_f (%)
Control	C1	-	-
Admixture	C2	Fly ash (20% cement replacement)	-
MicroFiber (PF8)	FT1	Polypropylene	0.1%
FM 150 (PF1)	FT2		
FM 300 (PF2)	FT3		
AntiCrack (GF1)	FT4	Glass	
Micro fiber (CF1)	FT5	Cellulose	
Microfiber (CF5)	FT6		

Table 2 - Detailed Test Results for Different Mixes

Mix/ Fiber Desig-nation	Fiber Type	Fiber Volume Fraction (%)	Average Area (mm^2)	Average Width (mm)	Max Width (mm)	No. of Cracks
C1	Control	0.0	305	2.17	2.77	2.3
PF1	FM 150	0.033	292	0.93	2.19	3
		0.066	317	1.87	3	2
		0.1	211	1.03	2.2	2
		0.3	11	0.12	0.5	0.3
PF2	FM 300	0.033	220	0.90	1.88	4
		0.066	400	1.65	3.1	2
		0.1	217	0.79	2.2	3
		0.3	195	0.83	2.28	2
PF3	FM MD	0.1	212	1.48	1.92	3.0
		0.2	59	0.52	0.54	2.0
		0.3	13	0.18	0.42	2.0
PF4	FM Stealth	0.1	121	1.02	1.32	2.0
		0.2	4	0.06	0.18	0.3
PF5	FM Stealth	0.1	216	1.16	1.32	3.7
		0.2	120	0.85	1.04	2.7
		0.3	102	0.68	0.89	7.0
PF6	FM Stealth	0.1	258	1.38	2.00	3.3
		0.2	243	1.32	1.42	3.0
		0.3	154	1.08	1.40	3.0
PF7	Fibrillated	0.1	173	0.93	1.02	2.7
		0.2	43	0.47	0.54	2.0
		0.3	31	0.34	0.38	1.3
PF8	Micro Fiber	0.033	158	1.11	1.94	1.3
		0.066	212	0.78	1.45	2.7
		0.1	31	0.31	0.43	0.3
CF1	Microfiber	0.033	394	1.64	2.8	2
		0.066	288	1.85	4	2
		0.1	198	0.56	1.86	3
		0.3	295	1.42	2.96	2
CF2	Microfiber	0.1	284	1.17	1.31	2.5
		0.2	240	1.72	2.74	2.0
		0.3	65	0.41	0.79	2.3
		0.4	27	0.27	0.60	0.7

Table 2 - (Continued)- Detailed Test Results of different mixes

Mix/Fiber Designation	Fiber Type	Fiber Volume Fraction (%)	Average Area (mm^2)	Average Width (mm)	Max Width (mm)	No. of Cracks
CF3	Microfiber	0.1	242	2.33	3.00	2.7
		0.2	230	1.83	2.50	1.7
CF4	Microfiber	0.2	280	2.00	2.50	2.5
		0.3	145	1.53	2.50	3.3
CF5	Microfiber	0.2	215	1.92	3.00	2.0
		0.4	10	0.10	0.31	0.3
GF1	Anti Crack fiber	0.033	56	0.54	1.02	1.0
		0.066	9	0.06	0.11	0.7
		0.1	0	0	0	0

Table 3- Fiber Properties

Fiber Designation	Fiber type	Length (mm)	Diameter (microns) or denier	Pictures
PF1	FM 150	Multi dimension (~7 to 20)	20 denier	
PF2	FM 300	Multi dimension (~15-20)	2600 denier	
PF8	MicroFiber	20	Microfilament	
GF1	AntiCrack fiber	18	Monofilament (14 microns)	
CF1	Micro fiber	2.1-2.5 (Sized)	18 (2.5 denier)	
CF5	Micro fiber	2-3	0.9-2.7 denier	

TEST METHODS

Restrained plastic shrinkage

The restrained plastic shrinkage tests were conducted using a technique developed by the authors. The technique developed by the authors involves placing the material being tested as an overlay above a substrate with standard roughness. Figure 1 shows a typical overlay cast over a substrate. The inset shows the protrusions on a typical substrate. The substrate provides realistic restraint to the overlay and this assembly is placed in an environmental chamber. In the environmental chamber a temperature of 50°C is chosen, which results in a relative humidity of less than 5% and this produces an evaporation rate of approximately 1.0 kg/m^2/h from the specimen surface. After 24hrs, cracking in the overlay (top inset Figure 1) is measured and the average crack width and total crack area is determined using a minimum of three specimens. Further details about this test technique have been previously published by the authors (Banthia & Gupta 2006; Banthia & Gupta 2007; Banthia & Gupta 2009) and is beyond the scope of this paper.

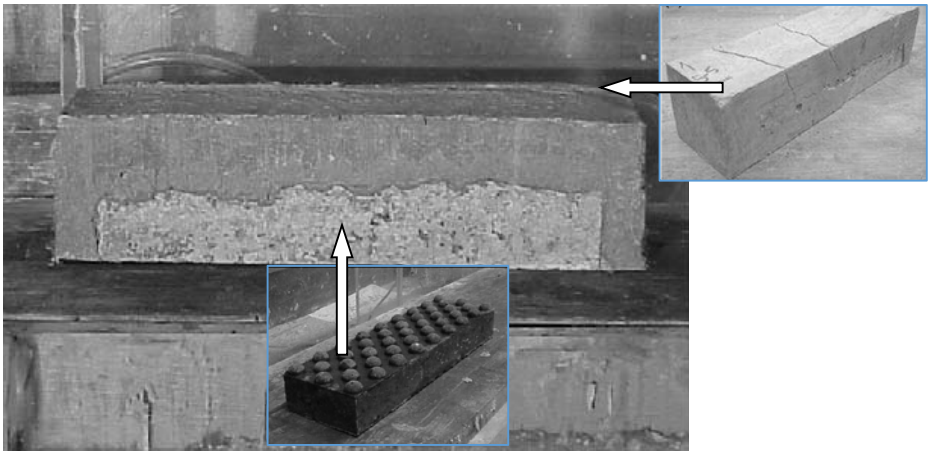

Figure 1. Specimen after demolding (bottom inset shows a typical substrate with protrusions and top inset shows cracked surface of overlay)

Compressive strength

Compressive strength of cementitious materials is the fundamental mechanical property that dictates the performance of the material under early age loading conditions. To evaluate early compressive strength, the control mix C1 was cast into 100 mm cube molds. Compressive strength of other fiber-reinforced mixes was expected to be similar, since all mixes had identical cement and water contents and nominal dosage of fibers. Test samples were cast and placed in the environmental chamber under the same temperature and relative humidity regime as used during the plastic shrinkage test method developed by the authors. Time to first crack for most mixes during restrained plastic shrinkage conditions was between 2-3 hrs. Hence, compressive tests were performed at approximately 3 hrs from the time of casting. These tests were performed using a closed-loop highly sensitive Instron Universal Testing Machine (model 8802). Load values along with cross-head displacements were recorded.

Tensile characteristics

As previously described, under restrained shrinkage conditions, cement based composites crack when the tensile stresses exceed the tensile strength of the material. The test described in this section was used to determine the enhancement in tensile strength of the material (if any) due to the addition of fibers at early ages and also to determine the effectiveness of the fibers to carry load after the first crack. This would also be indicative of the ability of fibers to inhibit crack growth under restrained shrinkage conditions.

Briquette specimens were cast using specially prepared molds (Figure 2) and were subjected to the environmental conditions similar to those experienced by the shrinking overlay in a typical shrinkage test. Briquette specimens were 25.4 x 25.4 mm in size at the critical cross section and the failure zone was 6 mm long. These briquettes have been previously used by Banthia et al. (1994, 1995) to perform tensile impact tests and they have also described the test set-up in detail. It should be noted that these tests require careful consideration of eccentricities that may be introduced during testing and the instability that is observed after the peak load.

Figure 2 - Molds for Casting Briquette Specimens

Tensile tests were conducted between 120 and 155 minutes from the time of casting corresponding to the time when restrained shrinkage cracks were expected to appear. Test equipment is shown in Figure 3. The equipment consisted of a fixed clamp and a moving clamp, which was connected to an LVDT and a load cell. The load cell had a capacity of

267 N and was sensitive enough to capture small load changes during testing. The deflection rate was controlled by changing the speed of the motor that powered the moving clamp. The initial speed was set at 0.3 mm/min till the first crack appeared (corresponding to the peak load) and was increased to 2.3 mm/min after the peak. The data was collected using a data acquisition system.

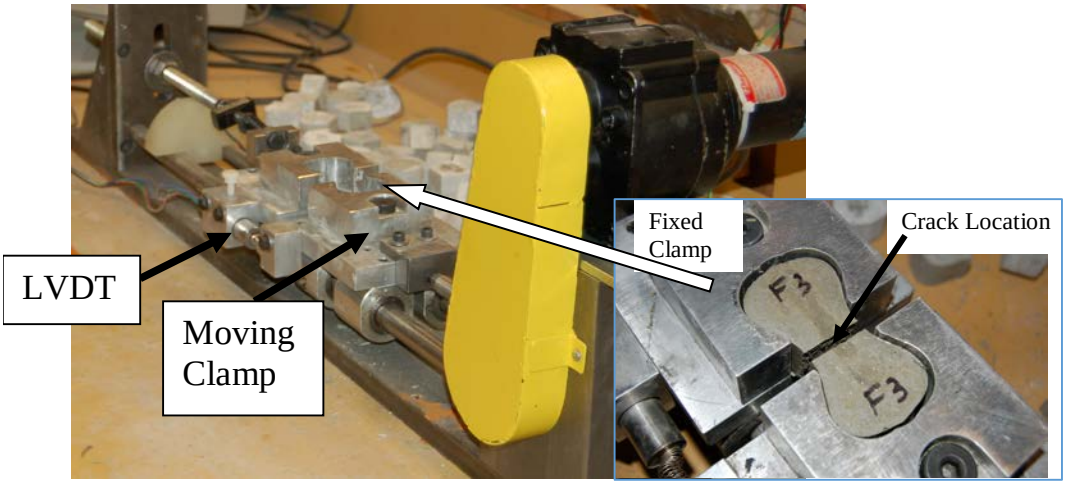

Figure 3 - Overall Arrangement for Uniaxial Tension Tests (inset showing details of the specimen during testing)

RESULTS (EARLY-AGE CHARACTERISTICS)

Compressive Strength

Elastic modulus (E) values along with the peak load and strength values are given in Table 4. Average compressive strength of the material was about 0.3 MPa and the elastic modulus was 2.14 MPa after 3 hrs of exposure in the environment chamber at 50°C. As expected, these values steadily increased with time indicating increased hydration and formation of a stronger microstructural skeleton. The peak stress increased by 48% in 25

minutes. The authors recognize that the reported values may be highly dependent on the loading surface characteristics and the rate of loading. These values, though approximate, present important information required for understanding the strength gain at early ages at elevated temperatures.

Table 4- Compressive Strength and Elastic Modulus at Early Ages

Time since casting (min)	Peak Load (kN)	Peak Stress (MPa)	Elastic Modulus "E" (MPa)
180	2.94	0.29	2.14
190	3.43	0.34	2.14
200	4.05	0.4	5.83
205	4.29	0.43	5.88

Uniaxial Tensile Properties

The load vs. deflection graphs for different mixes are plotted in Figures 4 to 7 and the test results have been summarized in Table 5. A typical failed specimen is shown in Figure 8, where pulled-out and fractured fibers across the crack can be noticed. The unsupported length at the start of the test was 6 mm and hence calculation of percent elongation was based on this length.

The load vs. deflection graphs for the five control samples tested are plotted in Figure 4. Some deviation in the peak load was observed depending on the location of the crack and the actual area of the cracked section. Peak tensile stress was calculated based

on measured areas and was found to be between 0.04 and 0.08 MPa. As expected no post peak ductility was observed due to lack of fibers. Test results for mix containing fly-ash are plotted in Figure 5, as expected the average tensile strength was 0.037 MPa, lower than that for control. In most specimens, some minimal initial non-linear strain was measured probably due to initial displacement between the specimen and the grips.

Load vs. deflection plots for the fiber reinforced mixes are plotted in Figures 5 to 7. It is evident that fibers added post peak load carrying capacity even at early ages suggesting their effectiveness in controlling propagation of cracks after their initiation. Tests were continued to a deflection, until fibers lost their load transfer capacity. Glass fibers had exceptional load carrying capacity with a plateau near the peak load indicating multiple cracking, strain hardening, and high effectiveness of fibers in controlling propagation of cracks.

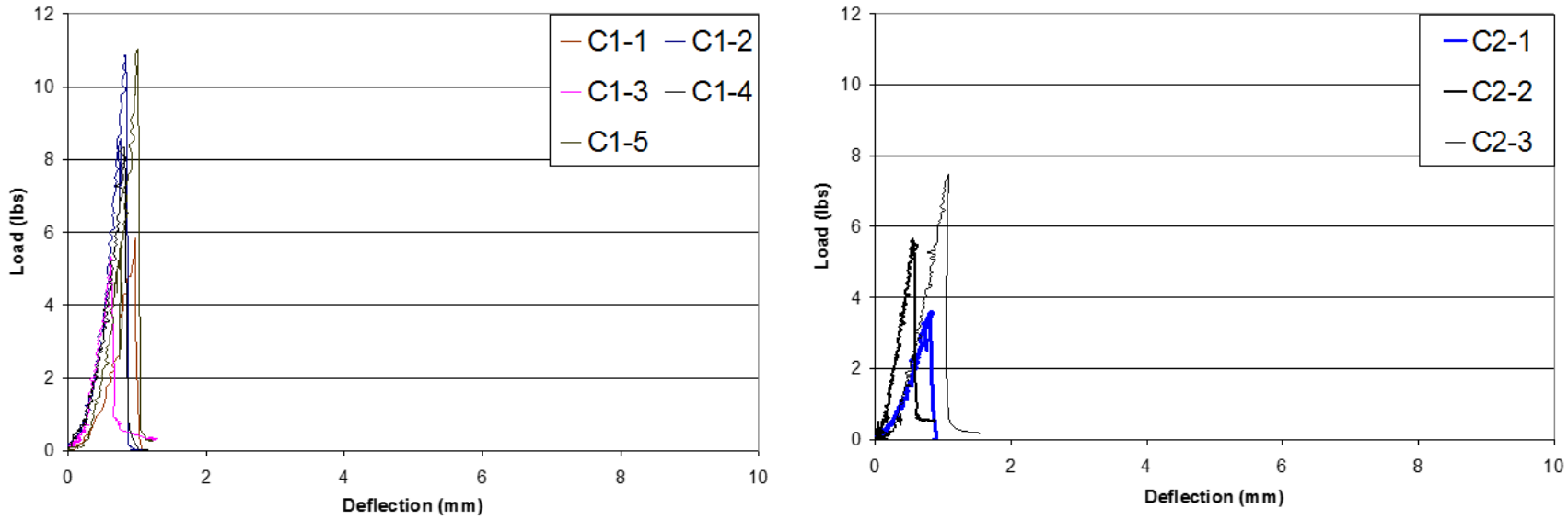

Figure 4 - Load vs. Deflection for control mixes: Mix C1 and Mix C2 (20% Fly-Ash)

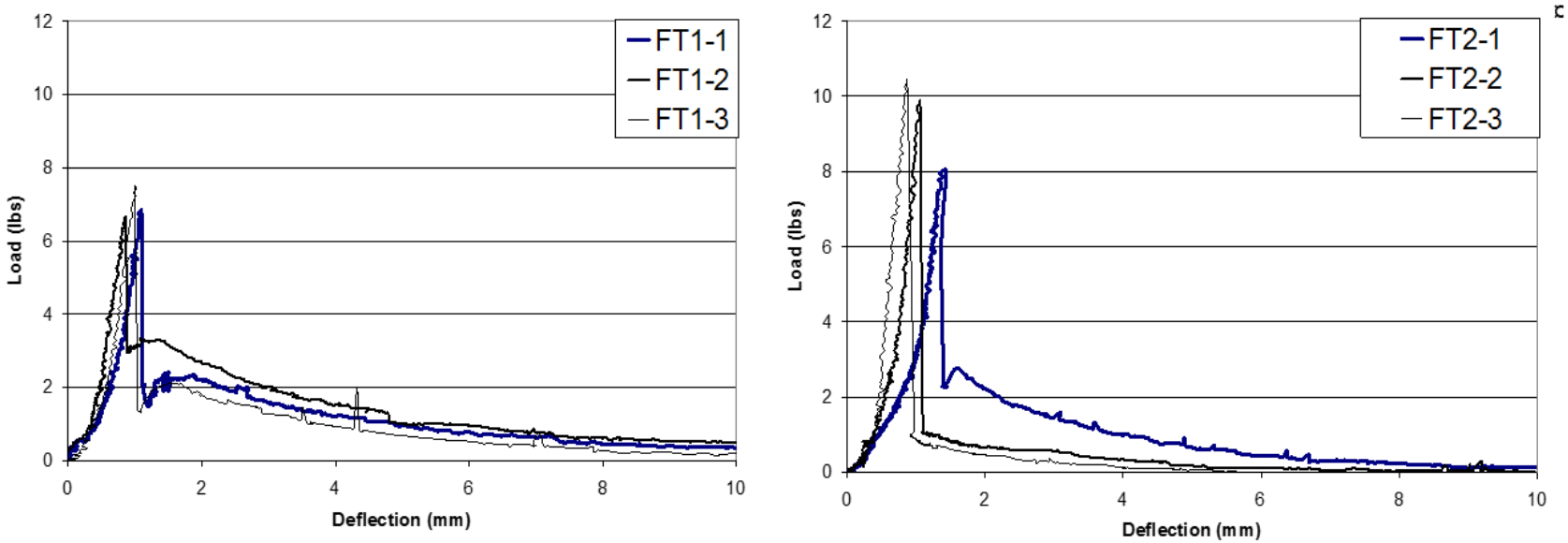

Figure 5 - Load vs. Deflection for Polypropylene fibers: Mix FT1 (Fiber PF8) & Mix FT2 (Fiber PF1)

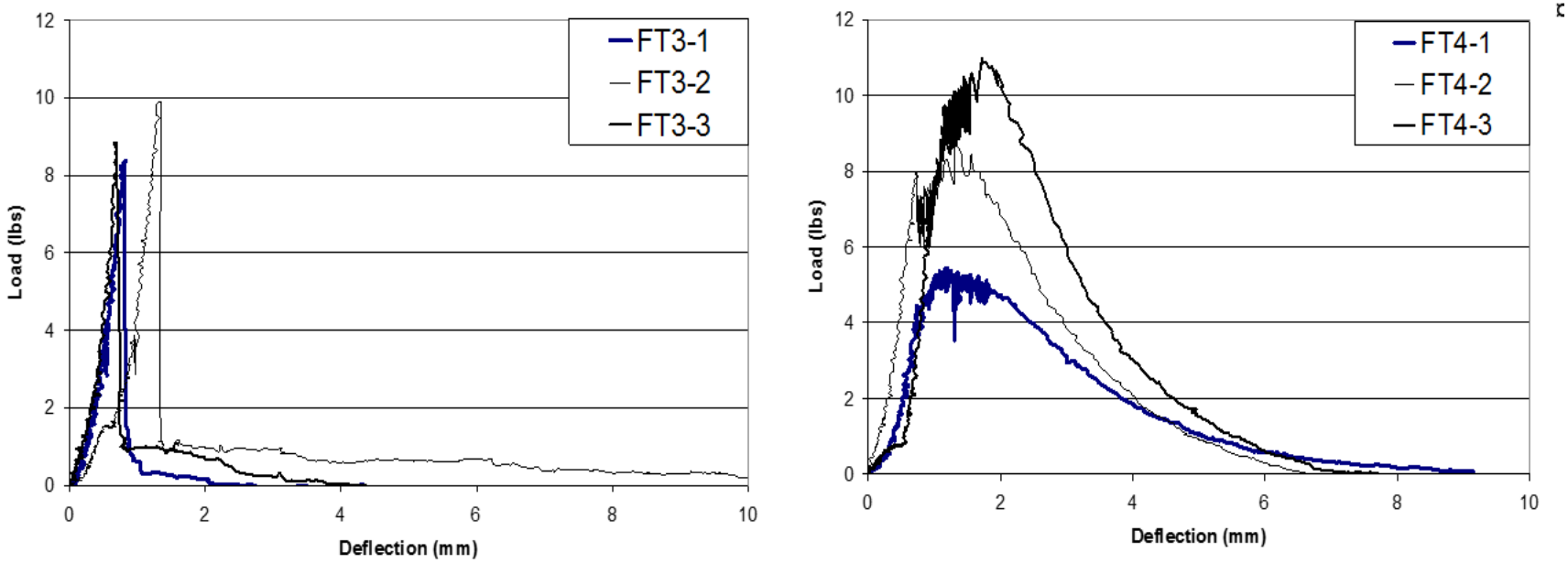

Figure 6 - Load vs. Deflection for Mix F3 (Polypropylene Fibers, PF2) & Mix F4 (Glass Fibers, GF1)

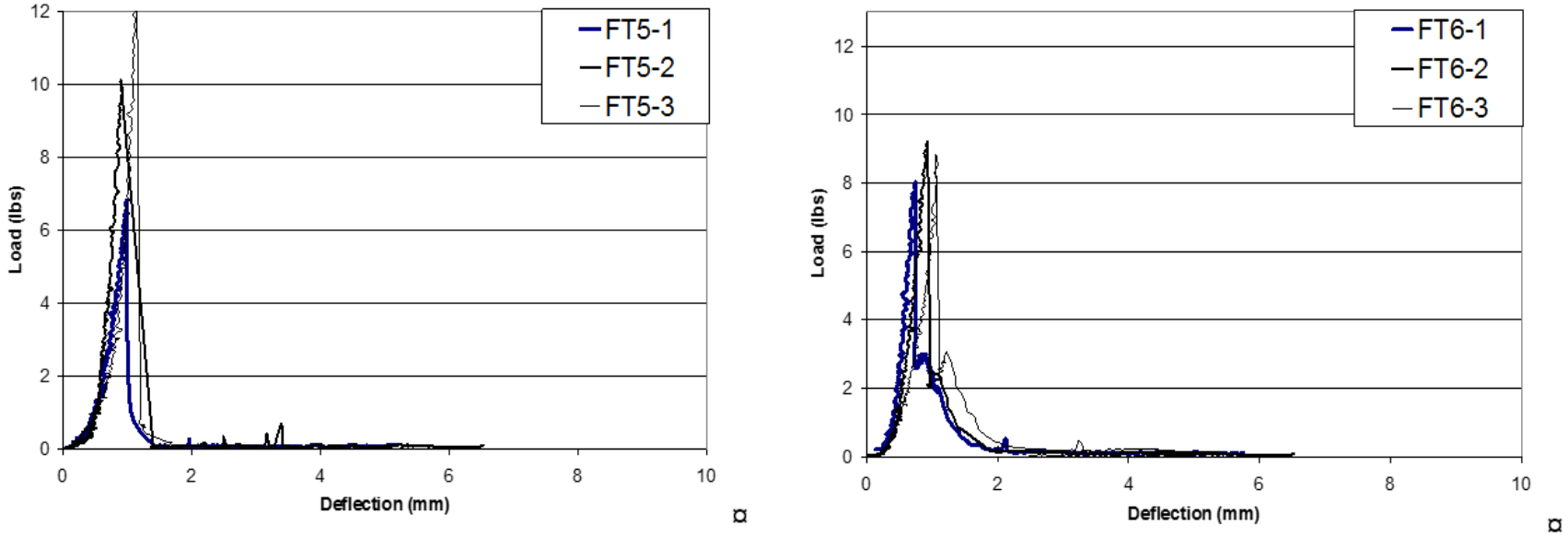

Figure 7 - Load vs. Deflection for Cellulose fibers: Mix F5 (Fiber, CF1) & Mix F6 (Fiber, CF5)

Figure 8 - A Tested Specimen Showing Polypropylene Fibers Across the Crack

The authors recognize that briquettes used for uniaxial tension suffer from load eccentricities causing the results to be a combination of tension and flexure. However, in the case of the tested fiber reinforced briquettes with large tensile ductility the specimens tend to correct alignment during loading due to the use of a universal joint and reduce eccentricity during a test.

ANALYSIS AND DISCUSSION

The load vs. deflection data was further analyzed and the following aspects were calculated:

- Peak tensile stress based on the maximum recorded load and the measured area at the failed cross-section. This stress represents the limit, which when exceeded will cause the first crack to appear in a shrinking overlay,

- Stress at 2 mm: Representing residual strength of the material at a typically observed crack width during a shrinkage test.
- Elongation at Peak: Representing the strain capacity of the material at the peak load even before a crack has appeared in the material. This value would indicate the effect of fibers and admixtures on the material's intrinsic strain capacity before cracking.

The above-mentioned properties of the various mixes are presented in Table 5 and graphically shown in Figure 9 where tensile stress at peak, at 2 mm deflection, and elongation at peak load in percentage are plotted.

Peak Stress: Average peak tensile stress for mix C2 was 0.037 MPa, 62% lower when compared to the control mix C1 due to the lower matrix strength. This was expected as the mix C2 contained 20% less cement, which was replaced with fly-ash that reduced the early-age matrix strength. Peak stress values for all fiber reinforced mixes were comparable to the control mix C1 (between 0.061 and 0.071 MPa) with the exception of mix FT1.

Stress Carried at 2 mm: Un-reinforced mixes had no residual strength at 2 mm deflection. Mixes (FT5 and FT6) containing cellulose fibers had marginal residual strength. Polypropylene fibers retained between 15 and 25% and the mixes ranked (in decreasing order): FT1 (fiber type PF8), FT2 (fiber type PF1), and FT3 (fiber type PF2).

In terms of residual strength at 2 mm, the most effective fibers were glass fibers (GF1) that retained 85% of its peak tensile strength even at a deflection of 2 mm. This

trend completely corroborated with the effectiveness of fibers in controlling crack area (at V_f = 0.1%) when mixes are exposed to restrained shrinkage conditions, hence indicating that residual strength under uniaxial tension is a good indicator of FRC performance under restrained plastic shrinkage conditions. For the same volume fraction, polypropylene fibers, PF1, which is a finer fiber as compared to PF2, indicated a much higher residual strength at 2 mm deflection and a higher percentage elongation at the peak.

Elongation at Peak: Percentage elongation at peak was calculated based on an unsupported specimen length of 6 mm. As seen in Figure 9, the elongation at peak for all unreinforced specimens was similar at about 13.5%. All fibers increased the strain capacity before reaching the peak load when compared to the unreinforced mixes. Marginal increase was observed with mixes FT1, FT3, FT5, and FT6. Polypropylene fiber mix FT2 and glass fiber mix FT4, on the other hand, increased the elongation at peak by more than 76% when compared to the control.

Table 5 - Uni-Axial Test Data

Material	Mix Designation	Testing Age (min)	Cracked area (mm^2)	Average Peak Load (N)	Average Tensile Stress (MPa)	Stress at 2 mm (MPa)	Elongation at Peak (mm)	% Elongation at Peak
Control	C1	130	614	37.3	0.060	0	0.8	13.5
Fly ash (20% cement replacement)	C2	132	672	25.0	0.037	0	0.8	13.6
Polypropylene (Grace)	FT1	137	648	31.2	0.048	0.015	1.0	16.4
Polypropylene (FM 150)	FT2	140	648	42.9	0.067	0.010	1.5	25.0
Polypropylene (FM 300)	FT3	135	624	40.1	0.064	0.004	0.9	15.8
Glass (Saint-Gobain)	FT4	137	624	38.4	0.061	0.052	1.4	23.8

Cellulose (Buckeye)	FT5	140	624	44.4	0.071	0.002	1.0	16.0
Cellulose (Weyerhaeuser)	FT6	130	624	39.2	0.063	0.003	0.9	15.3

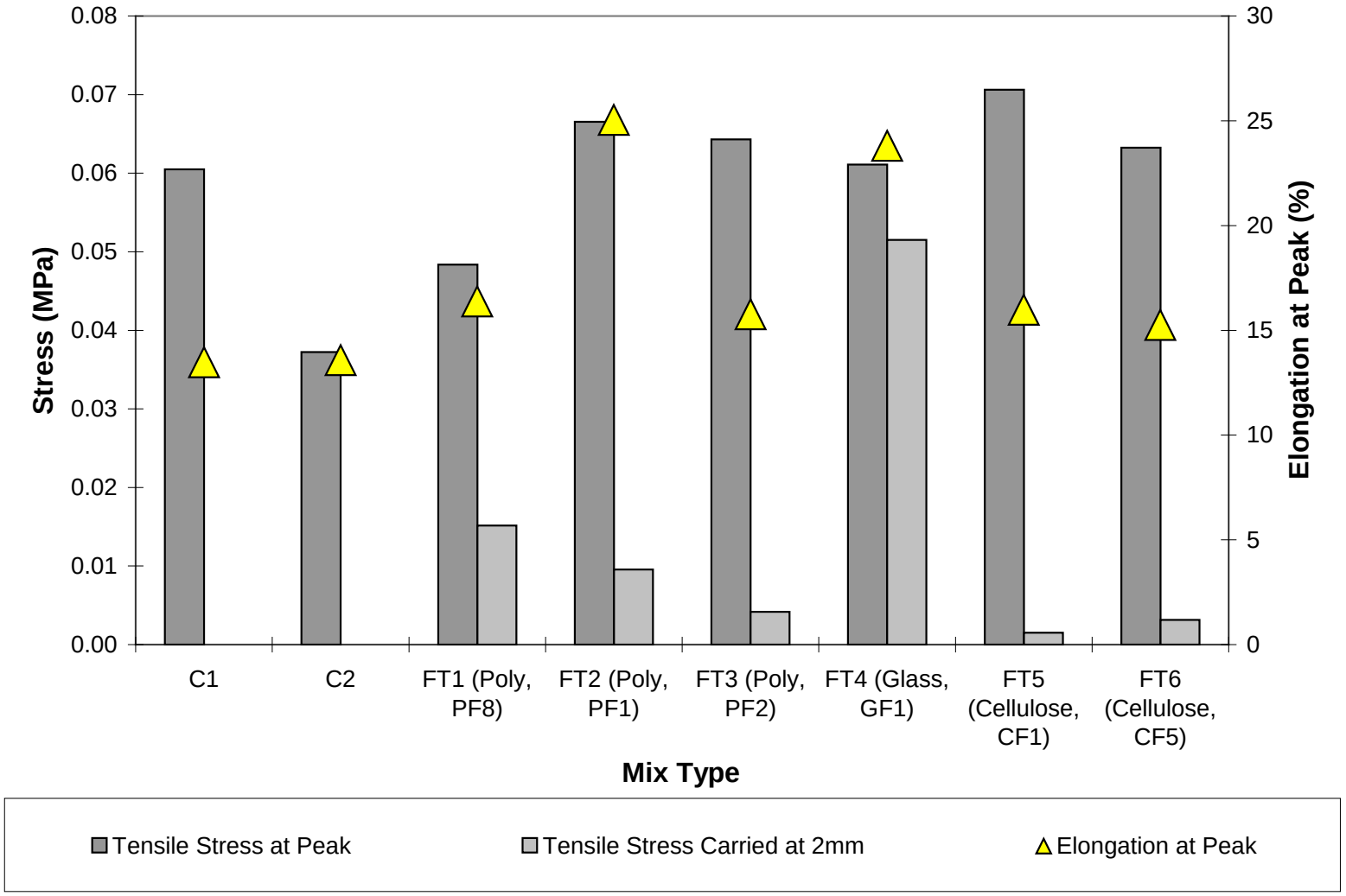

Figure 9 - Stress and Elongation for Different Mixes

Discussion: This study clearly indicated that certain fibers are effective in only marginally increasing the tensile strength of the material itself and some increase both the residual strength and elongation capacity at early ages. Fly-ash reduces the early-age tensile strength of the material and would thus be expected to increase restrained plastic shrinkage cracking. In general, glass fibers were found to be the most effective followed by polypropylene fibers and the cellulose fibers. These findings are in complete agreement with the effect of these fibers on shrinkage cracking. In Figure 10 a plot showing comparison of tensile stresses carried at 2 mm (recorded from briquette specimens) and shrinkage crack area recorded from testing for mixes containing identical fiber dosage is made. It can be clearly seen that for most fibers, an increase in the tensile strength at 2 mm reduced the shrinkage cracking potential. Amongst the various properties investigated, residual strength was the most effective parameter in indicating effectiveness of fibers to mitigate restrained plastic shrinkage cracking.

The uniaxial tests described above are one of the first attempts in quantifying the performance of early age properties of fiber-reinforced cement-based materials especially at early ages, after they have been exposed to severe conditions of drying that is conducive to shrinkage cracking. Limited studies report work similar to the one described above (Komlos 1979, Kovler 1994, Kovler & Bentur 1997).

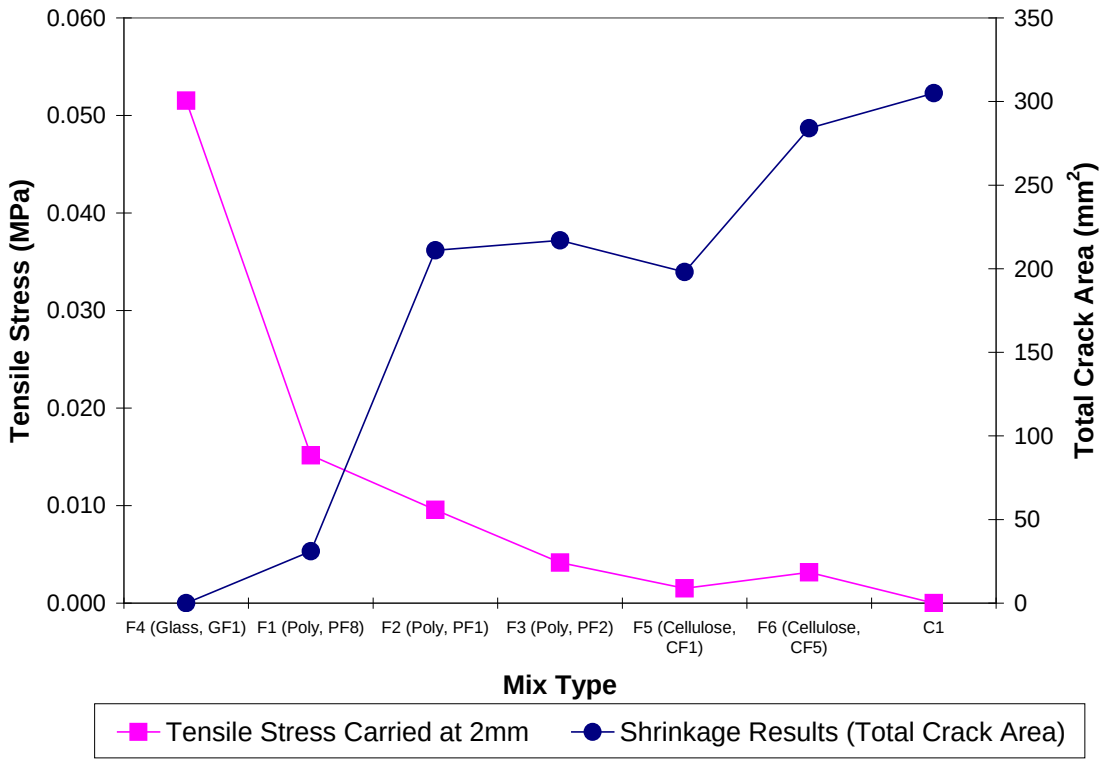

Figure 10 - Comparison of Tensile Stress at 2 mm and Shrinkage Cracking

Concluding remarks

Uniaxial tensile tests on young fiber reinforced mortar specimens clearly indicated that certain fibers are effective in marginally increasing the tensile strength of the material itself and some increase both the post-peak residual strength and elongation capacity. Fly-ash reduces the early-age tensile strength of the material and would thus be expected to increase restrained plastic shrinkage cracking. From the uniaxial tests, glass fibers were found to be the most effective followed by polypropylene fibers and cellulose fibers. These findings are in agreement with the effect of these fibers on shrinkage cracking. Amongst the various properties investigated using the uniaxial tests, residual strength was the most effective in

relating effectiveness of fibers in improving uniaxial tensile properties to behavior of material under restrained plastic shrinkage conditions.

Acknowledgements

The authors acknowledge the financial support of NSERC Canada and the involvement of various undergraduate and visiting graduate students.

REFERENCES

Akcay, B. (2012). Experimental investigation on uniaxial tensile strength of hybrid fibre concrete. Composites Part B, 43(2), 766-778. doi:10.1016/j.compositesb.2011.08.017

Aly, T., & Sanjayan, J. G. (2010). Shrinkage-cracking behavior of OPC-fiber concrete at early-age. Materials and Structures, 43(6), 755-764. doi:10.1617/s11527-009-9526-7

ASTM C 1579 (2006). Standard Test Method for Evaluating Plastic Shrinkage Cracking of Restrained Fiber Reinforced Concrete (Using a Steel Form Insert). *American Society of Testing and Materials,* Philadelphia.04.02.

Banthia, N., Azzabi, M. and Pigeon, M. (1993). Restrained Shrinkage Cracking in Fiber Reinforced Cementitious Composites. *Materials and Structures.* RILEM (Paris), 26 (161). 405-413.

Banthia, N., Chokri, K., Ohama, Y., and Mindess, S. (1994). Fiber-Reinforced Cement Based Composites Under Tensile Impact. *Advanced Cement Based Materials*, 1, 131-141.

Banthia, N. & Gupta, R. (2006). Influence of Polypropylene Fiber Geometry on Plastic Shrinkage Cracking in Concrete, *Cement and Concrete Research*, 36(7), 1263-1267

Banthia, N. & Gupta, R. (2007). Test Method for Evaluation of Plastic Shrinkage Cracking in Fiber Reinforced Cementitious Materials, *Experimental Techniques*, 44-48.

Banthia, N., Gupta, R. (2009). Plastic Shrinkage Cracking in Cementitious Repairs and Overlays, *Materials and Structures*, 42, 567-579

Banthia, N., Moncef, A., Chokri, K., and Sheng, J. (1995). Uniaxial tensile response of microfiber reinforced cement composites. *Materials and Structures*, 28, 507-517.

Bayasi, Z., and McIntyre, M. (2002). Application of Fibrillated Polypropylene Fibers for Restraint of Plastic Shrinkage Cracking in Silica Fume Concrete. *ACI Materials Journal*, 99 (4), 337-344.

Bloom, R. and Bentur, A. (1995). Free and Restrained Shrinkage of Normal and High Strength Concrete. *ACI Materials Journal*, 92 (2), 211-217.

Grzybowski, M. and Shah, S.P. (1990). Shrinkage Cracking of Fiber Reinforced Concrete. *ACI Materials Journal*, 87 (2), 138-148.

Gupta, R. (2008). Development, application and early-age monitoring of fiber-reinforced 'crack-free' cement-based overlays", Doctoral thesis , University of British Columbia, Vancouver, Canada.

Khajuria, A. and Balaguru, P. (1992). Plastic Shrinkage Characteristics of Fiber Reinforced Cement Composites. *Fiber Reinforced Cement and Concrete* (Ed. R.N. Swamy), E&FN Spon, London, 82-90.

Komlos, K. (1979). Uniaxial tensile strength of early age fibre concretes. *Mater Constr Mater Struct*, 12 (69), 201-206.

Körmeling, H. A., & Reinhardt, H. W. (1987). Strain rate effects on steel fibre concrete in uniaxial tension. International Journal of Cement Composites and Lightweight Concrete, 9(4), 197-204. doi:10.1016/0262-5075(87)90002-9

Kovler, K. (1994). Testing system for determining the mechanical behaviour of early age concrete under restrained and free uniaxial shrinkage. *Materials and Structures*, 27, 324-330

Kovler, K. (1995). Interdependence of creep and shrinkage for concrete under tension. *ASCE Journal of Materials in Civil Engineering*, 7 (2), 96-101.

Kovler, K., Bentur, A. (1997). Shrinkage of early age steel fiber reinforced concrete. *Archives of Civil Engineering*, 43 (4), 431-439.

Kronlof, A., Markku; L., Pekka, S. (1995). Experimental study on the basic phenomena of shrinkage and cracking of fresh mortar. *Cement and Concrete Research*, 25 (8), 1747-1754.

Lura, P., Pease, B., Mazzotta, G. B., Rajabipour, F., Weiss, J. (2007). Influence of Shrinkage-Reducing Admixtures on Development of Plastic Shrinkage Cracks. *ACI Materials Journal*, 104 (2), 187-194.

Meng, Y., Chengkui, H., & Jizhong, W. (2006). Characteristics of stress-strain curve of high strength steel fiber reinforced concrete under uniaxial tension. Journal of Wuhan University of Technology. Materials Science Edition, 21(3), 132-137. doi:10.1007/BF02840902

Naaman, A. E., Wongtanakitcharoen, T., and Hauser, G. (2005). Influence of Different Fibers on Plastic Shrinkage Cracking of Concrete. *ACI Materials Journal*, 102 (1), 49-58.

Qi, C., Weiss, J., and Olek, J. (2003). Characterization of plastic shrinkage cracking in fiber reinforced concrete using image analysis and a modified Weibull function. *Materials and Structures*, 36 (260), 386-395.

Qi, C., Weiss, W. J., and Olek, J. (2005). Assessing the settlement of fresh concrete using a non-contact laser profiling approach. *International Conference on Construction Materials: ConMat'05*, Vancouver, Canada.

Slowik, V., Schlattner, E., and Klink, T. (2004). Experimental investigation into early age shrinkage of cement paste by using fibre Bragg gratings. *Cement and Concrete Composites: Early Age Concrete - Properties and Performance,* 26(5), 473-479.

Soroushian, P., Mirza, F., Alhozajiny, A. (1993). Plastic Shrinkage Cracking of Polypropylene Fiber Reinforced Concrete. *ACI Materials Journal,* 92 (5), 553-560.

Topcu, I. B., and Elgun, V. B. (2004). Influence of concrete properties on bleeding and evaporation. *Cement and Concrete Research*, 34 (2), 275-281.

Trottier, J-F, Mahoney, M, and Forgeron, D. (2002). Can Synthetic Fibers Replace Welded-Wire Mesh in Slabs-on-Ground? *Concrete International*, 24 (11), 59-68.

Wille, K., El-Tawil, S., & Naaman, A. E. (2014). Properties of strain hardening ultra high performance fiber reinforced concrete (UHP-FRC) under direct tensile loading. Cement and Concrete Composites, 48, 53-66. doi:10.1016/j.cemconcomp.2013.12.015